Nano Hybrids and Composites
ISSN: 2297-3400, Vol. 27, pp 21-29
doi:10.4028/www.scientific.net/NHC.27.21

Submitted: 2019-08-06
Revised: 2019-11-15
Accepted: 2019-11-15
Online: 2019-11-29

Ni-Doped ZnO Thin Films Deposited by Pneumatic Spray Pyrolysis

L. Herissi[1,2,a*], L. Hadjeris[2], M.S. Aida[3], S. Azizi[2], A. Hafdallah[1] and A. Ferdi[1]

[1]Larbi Tebessi University - Tebessa, Algeria

[2]LMSSEF, Oum El Bouaghi University, 04000, Algeria

[3]Departement of Physics, King Abdulaziz University, Saudi Arabia

[a]hlabidi12@gmail.com, l.herissi@univ-tebessa.dz

Keywords: Thin films; Pneumatic spray pyrolysis; Doping effect; Optical properties; Electrical conductivity.

Abstract. The objective of the present work is the study the Ni concentration effect on the optical, structural and electrical properties of ZnO:Ni thin films deposited by pneumatic spray pyrolysis method. Un-doped and Ni-doped ZnO thin films were prepared from zinc acetate dihydrate and nickel chloride hexahydrate dissolved in distilled water onto glass substrates by pneumatic spray pyrolysis method. Solution concentration, substrate temperature and nozzle-substrate distance were kept constant during all deposition processes. Effect of nickel content on the optical, structural and electrical properties of as-prepared films obtained was investigated by UV–Vis-NIR spectrophotometry, X-ray diffraction and four-point probe technique. The results indicate that the deposited films are well adherent to the substrates, present surface roughness and have a preferential growth in the (002) direction. The observed transmittance in the visible region was situated between 60% and 70%. For Ni-doped ZnO, there are two separate phases. The Urbach energy, grain size, and electrical conductivity increase with Ni content. The same behavior for both the optical energy gap and the ZnO:Ni lattice parameters.

Introduction

The activity "semiconductor oxides" is centered on zinc oxide (ZnO) and nickel oxide (NiO), and their alloys [1-6]. ZnO and NiO are n-type group II-VI semiconductor and p-type group VIII-VI semiconductor, respectively, although they both have wide optical gap at room temperature [2,7].

Several authors have characterized the Ni doped ZnO thin films [3,4,8-11] and Zn doped NiO thin films [2,5,6] elaborated by several techniques such as: pulsed laser deposition [3,12], sol–gel method [4-6,10,11], chemical bath deposition [8], and spray pyrolysis technique [2,9]. They also studied the variation of their properties as a function of deposition conditions such as doping concentration, nature and temperature of the substrate, technique of deposition and the nature of the chemical precursor used to control, in principle, the phase deposited and its morphology. On the other hand, the deposition of thin films from spray pyrolysis methods catches the attention of researchers because these methods have several advantages, namely: cost effectiveness, low-cost setup, flexibility over the conventional plasma film deposition methods, and vacuum-less equipments [2].

The objective of the present work is the characterization of the ZnO:Ni thin films deposited onto glass substrates by pneumatic spray pyrolysis method to determine the Ni concentration effect on their optical, structural and electrical properties because the zinc oxide thin films doped by transition metals have a lot of applications in optoelectronic devices such as solar cells, flat panel displays, photodetectors, gas sensors, and spintronics, They also show room temperature ferromagnetism without carrier incorporation, through double exchange mechanism [2,4,8-13].

Experimental Procedure

ZnO:Ni thin films were deposited onto glass substrates from zinc acetate dihydrate and nickel chloride hexahydrate dissolved in distilled water by pneumatic spray pyrolysis technique (PSP) using an air compressor (Fig. 1). Solution concentration, substrate temperature and nozzle-substrate

distance were kept constant during the whole deposition process at 0.05 mol/l, 350 °C and 30 cm, respectively. Different Ni atomic concentration (x ratio) were used and controlled through the variation of the solution concentration of precursor sources of nickel and zinc separately with x = [Ni]/[Ni+Zn] = 0, 5, 10, and 15 at. %. An estimated deposition time leading to a constant film thickness was retained [2]. The characterization of the deposited films were performed in ambient atmosphere at room temperature.

The UV–Vis-NIR transmittance T(λ) of the films on glass substrates was measured using a double-beam spectrophotometer JASCO V-630. The film structure was investigated by X-ray diffraction (XRD) model Thermo Scientific ARL EQUINOX 100 X-ray Diffraction that measures all diffraction peaks simultaneously and in real time at 41 kV, 0.9 mA with a filtered Cu:$K_{\alpha 1}$ radiation (λ = 1.54056 Å). The film conductivity was determined from the sheet resistance measurement by a four-point probe technique (A Jandel cylindrical four-point probe head and Keithley Current Source Model 2400).

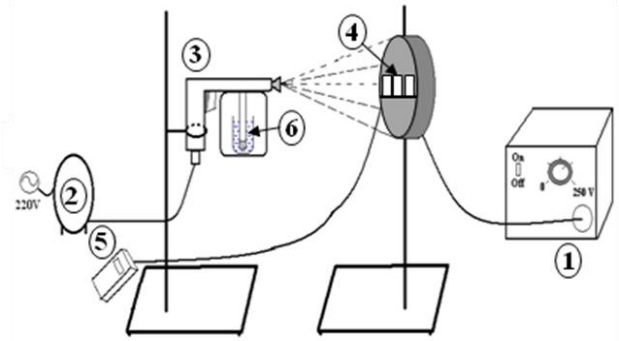

Fig. 1. Experimental device used to deposit ZnO:Ni thin films;
1. Power supply, **2.** Air compressor, **3.** Spray gun, **4.** Glass substrates on an electrical hotplate, **5.** Digital thermocouple, **6.** Solution to deposit.

Results and Discussion

Optical properties. All the obtained thin films were transparent and well adherent to the substrate. Fig. 2 shows the variation of optical transmittance spectra with wavelength for ZnO:Ni thin films deposited by PSP technique for different Ni content. All the transmission spectra obtained in our films are similar to each other, they are slightly sensitive to the variation of the Ni concentration, and they have a good optical transmittance situated between 60 % and 70 % in the Vis-NIR region. The optical transmission of the deposited films decreases with the decreasing wavelength in Vis-NIR region and interference fringes are not observed. This can be explained by oxygen deficiency in the material and the surface roughness of the thin films [1,2,14-16].

As can also be observed on all the measured transmission spectra, there is a decline of the curves at 380 nm wavelength which represents the intrinsic absorption characteristic of the pure ZnO and/or doped ZnO gaps deposed by spray pyrolysis technique using aqueous solutions of zinc acetate dihydrate [2,17-19]. Other than, a second decline is observed at 330 nm for doped ZnO films prepared at x =5, 10, and 15 at. %, that indicates the presence a second separate phase [2,17].

From these spectra (Fig. 2), we also deduced values of certain optical parameters such as: optical energy gaps (E_g), Urbach energy parameter (E_{Urb}), refractive index ($n(\lambda)$) and film thickness (d). In this work, the film thickness was calculated by Swanepoel's envelope method [15,20,21]. An average value ($d \approx 0.4\mu m$) was obtained.

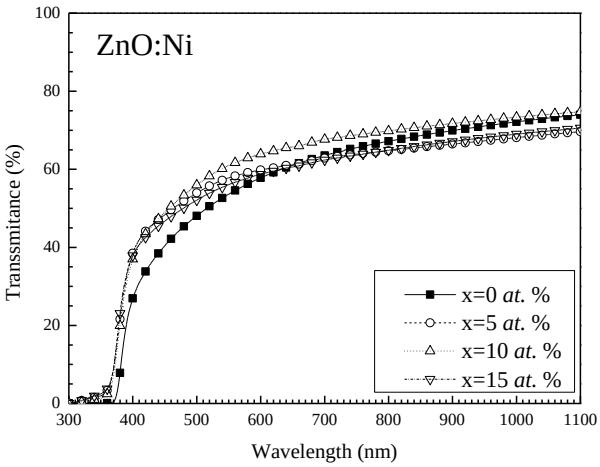

Fig. 2. Spectral variation of transmittance for ZnO:Ni films prepared for different x ratios by pneumatic spray pyrolysis.

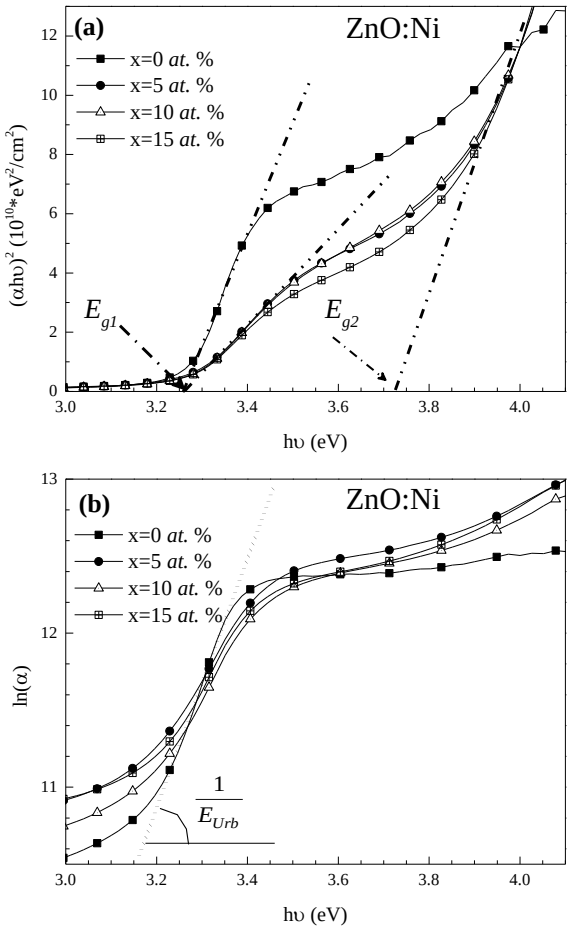

Fig. 3. The dependence of $(\alpha h\upsilon)^2$ and ln(α) on the incident photon energy (hυ) for ZnO:Ni.

The optical energy gaps and the Urbach energy parameter are obtained (Fig. 3) using Tauc's formula (Eq.1) for direct band gap semiconductors and Urbach's formula (Eq.2) respectively [11,12,18]:

$$(\alpha h\upsilon)^2 = A(h\upsilon - E_g) \quad (1)$$

$$\ln \alpha = \left(\frac{1}{E_{\mathrm{Urb}}} \right) h\upsilon + \ln \alpha_0 \tag{2}$$

where A is a constant depending on the electron–hole mobility, h is the Planck's constant, υ is the frequency of the incident radiation, and α is the absorption coefficient deduced from the measured transmittance T (%) using Beer–Lambert law [2,14]:

$$\alpha = \frac{1}{d} \ln \left(\frac{100}{T(\%)} \right) \tag{3}$$

Fig. 4 shows the variation of the optical gap energy with Ni concentration. For x = 0, the optical gap value agrees with the optical gap of ZnO [1,2,9,11]. For $x \neq 0$, the two optical gaps values (E_{g1} and E_{g2}) are deduced from two linear parts of the spectrum of $(\alpha h\upsilon)^2$ as a function of incident photon energy ($h\upsilon$) (Fig. 3.a), indicating the presence of two separate phases [2]. The values of E_{g1} lie between 3.26 and 3.27 eV which is in good agreement with the interval values (3.1-3.5 eV) of the reported ZnO and/or doped ZnO [1,2,17,18]. E_{g2} values vary between 3.72 and 3.75 eV which is in good agreement with the declared NiO band gap interval values of 3.15-3.80 eV when deposed by spray pyrolysis technique using aqueous solutions of nickel chloride at different conditions [2,22-24]. On the other hand, when the Ni concentration increases, E_{g1} decreases and E_{g2} increases as observed in previous work [2].

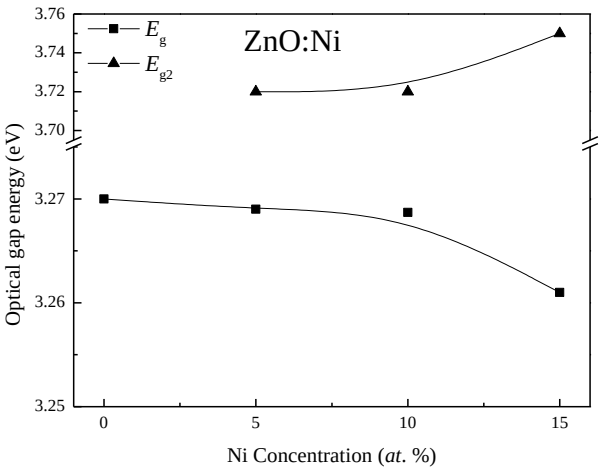

Fig. 4. Variation of the optical gap energy (E_g) with Ni concentration of ZnO:Ni films.

Fig. 5. shows the variation of the Urbach energy with Ni content in the solution. For x = 0, the E_{Urb} is smaller (23.34 meV) than for $x \neq 0$ (≈110 meV), because the un-doped ZnO films have less impurities, defects and less disorder owing to an almost complete chemical decomposition [1,18], when the nominal fraction of Ni increases in the precursor solution, the second separate phase (NiO) appears which causes the increase in the band tails [2].

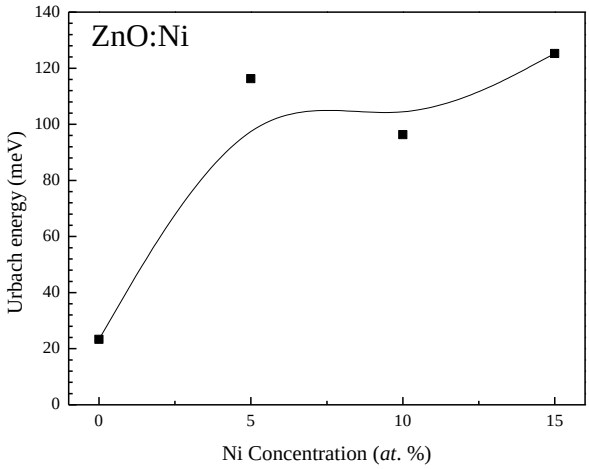

Fig. 5. Variation of the Urbach energy (E_{Urb}) with Ni concentration of ZnO:Ni films.

Structural properties. From the X-ray diffraction patterns shown in Fig. 6, the all films deposited by pneumatic spray pyrolysis from zinc acetate dihydrate and nickel chloride hexahydrate solutions dissolved in distilled water are polycrystalline. It was seen that undoped and Ni-doped ZnO samples exhibit peaks corresponding to (100), (002), (101), (102), (110), (103), and (112) planes, the peaks of all XRD patterns show no trace of nickel or its oxide. It may therefore be concluded that Ni^{2+} ions are incorporated into the wurtzite structure of ZnO at the Zn^{2+} sites [3,4,5,8,13]. The appearance of NiO secondary phase is due to the limited solid solubility of Ni in ZnO host matrix [9,13,25], The NiO phase does not appear in the XRD patterns can be interpreted by a few amount of NiO phase compared to the ZnO phase.

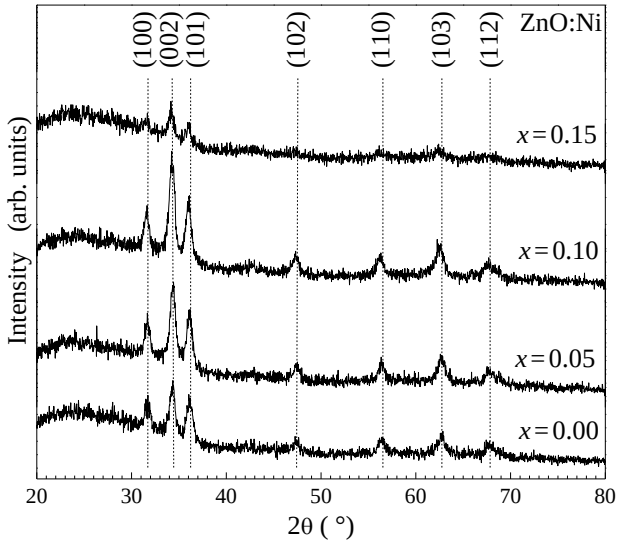

Fig. 6. X-ray diffraction for ZnO:Ni films prepared for different x ratios by pneumatic spray pyrolysis.

From the texture coefficient of the mille indices (*hkl*) plane $TC(hkl)_j$ evaluated from Equation 4 [14,15], the preferred orientation of the all films is (002), which suggests that the c-axis is perpendicular to the substrate surface and have a hexagonal crystal structure [8,9].

$$TC(hkl)_j = \frac{I(hkl)_j / I_0(hkl)_j}{\frac{1}{n}\sum_{i=1}^{n}\left[I(hkl)_i / I_0(hkl)_i\right]} \quad (4)$$

where n is the number of the diffraction peaks, I(*hkl*) and I_0(*hkl*) is the measured intensity and the JCPDS standard intensity data of the corresponding powder for (*hkl*) plane [19], respectively.

The grain size of the peak corresponding (*hkl*) plane " D_{hkl} " is calculated using the Scherrer's formula [11,12,15] :

$$D_{hkl} = \frac{0.94\,\lambda}{\beta.\cos\theta_{hkl}} \tag{5}$$

where λ is the wavelength of X-ray used for diffraction, β is the full width at half maximum (FWHM) of the diffraction peak and θ_{hkl} is Bragg's angle.

Fig. 7 shows the variation of D_{100}, D_{002}, and D_{101} as a function of the Ni content in solution of precursor sources deposited at 350 °C and 0.05 M. Considering several scientific works [2,8,13], we can note that all the grains increase when the nominal fraction of Ni increases in the precursor solution. This proves that there are Ni ions go in the interstitial positions in the crystalline structure of the ZnO which also explains the increase of the band tails (Fig.5) [8,13]. However, El-Hilo et al. who interpreted that the formation of NiO grains by there are the part of Ni ions did not enter in the crystalline structure of ZnO due to the limitation of the solid solubility of Ni in ZnO [13].

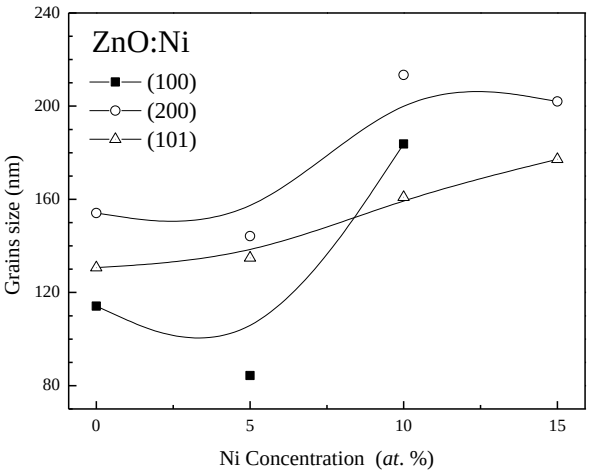

Fig. 7. Variation of the grains size of ZnO:Ni.

The lattice parameters (*c*, *a*) of ZnO:Ni are calculated using formulas for the hexagonal crystal (Eq.6, Eq.7, or Eq.8) of ZnO from the XRD data by three peaks related to the (100), (002) and (101) planes :

$$c_{ZnO} = \frac{\lambda}{\sin\theta_{002}} \tag{6}$$

$$a_{ZnO} = \frac{\lambda}{2.\sin\theta_{100}} \tag{7}$$

$$a_{ZnO} = \frac{2.\lambda.c}{\sqrt{12.c^2.\sin^2\theta_{101} - 3.\lambda^2}} \tag{8}$$

The lattice parameters variation with nominal Ni doping concentrations of (Zn,Ni)O for x = 0, 5, 10, and 15 at. % present in Fig. 8.

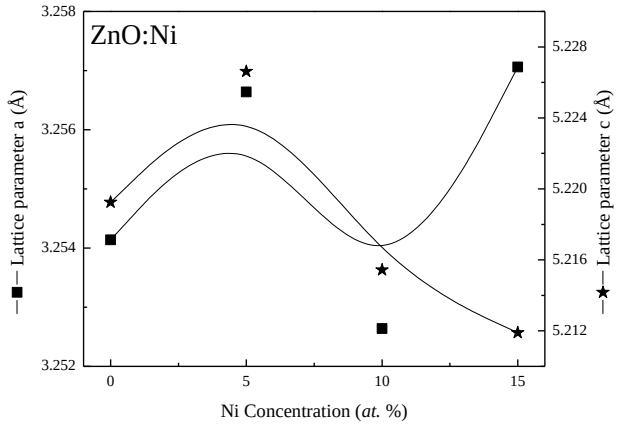

Fig. 8. Variation of the Wurtzite lattice parameters of ZnO:Ni.

As can be seen, the experimental values c = (5.218±0.004) Å and a = (3.255±0.001) Å are bigger than the standard values (c_0 = 5.206 Å and a_0 = 3.245 Å). Although, There is a slight decrease in lattice parameters (a and c) with increase of nickel atomic concentration from x = 0 to 10 *at*. %. This decrease is caused by partial occupation ionic radius of Zn ($r_{Zn^{+2}} = 0.74\,\text{Å}$) sites by smaller ionic radius of Ni ($r_{Ni^{+2}} = 0.69\,\text{Å}$) that indicates Ni doping in ZnO crystalline structure and also confirms the decrease in the Band gap energy [2,3,9,12,13]. For x = 15 *at*. %, the increase of c-parameter leads to the large increase of the optical energy gap of second phase (ΔE_{g2} = 0.03 eV) by comparison to its decrease for the first phase (ΔE_{g1} = 0.008 eV) [12].

Electrical properties. Electrical conductivity of ZnO:Ni thin films were measured by the four point probe method whose principle is to inject a current (I) at the two extreme points and to measure the voltage (V) at the of the two internal points. Therefore, the electrical conductivity in the case of an equally spaced in-line four point geometry is related to the thickness of the films by the following expression [26] :

$$\sigma = \frac{\ln 2}{\pi . d} . \frac{I}{V} \tag{9}$$

Fig. 9 shows the evolution of the electrical conductivity as a function of the Ni content. The increase of electrical conductivity is related with the grain size and leads to a decrease in grain boundaries, which contributes to increasing the mobility of the charge carriers [1,2,3,17,18]. On the other hand, as can be interpreted as more electrons with increase of Ni atomic percentage in ZnO thin films promoted to the conduction band [25].

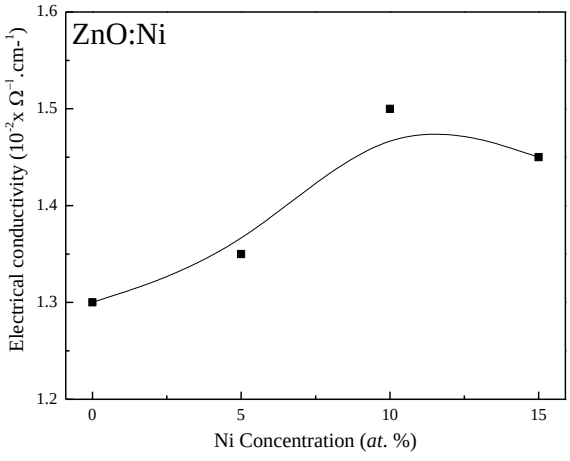

Fig. 9. Variation of the electrical conductivity of ZnO:Ni.

Conclusion

ZnO:Ni thin films were prepared from zinc acetate dihydrate and nickel chloride hexahydrate dissolved in distilled water onto glass substrates by pneumatic spray pyrolysis method. An estimated deposition time leading to a film thickness of about 0.4 μm was retained. The deposited films were transparent in the Vis-NIR region, well adherent to the substrates and present surface roughness. These studies indicate that for Ni-doped ZnO, there are two optical gaps values (*3.3 eV* and *3.7 eV*) indicating the presence of two separate phases (ZnO:Ni and NiO), the appearance of NiO secondary phase is due to the limited solid solubility of Ni in ZnO host matrix. The same behavior is observed for both the optical energy gap and the ZnO:Ni lattice parameters. With increasing the Ni content in the solution of precursor sources, Urbach energy, grain size and electrical conductivity are increased.

References

[1] L. Herissi, L. Hadjeris, H. Moualkia, N. Abdelmalek, N Attaf, M. S. Aida, J. Bougdira, Realization and study of ZnO thin films intended for optoelectronic applications, J. New Technol. Mater. 1 (2011) 39–43.

[2] L. Herissi, L. Hadjeris, M.S. Aida, J. Bougdira, Properties of $(NiO)_{1-x}(ZnO)_x$ thin films deposited by spray pyrolysis, Thin Solid Films, 605 (2016) 116–120.

[3] S. Thota, L.M. Kukreja, J. Kumar, Ferromagnetic ordering in pulsed laser deposited $Zn_{1-x}Ni_xO$/ZnO bilayer thin films, Thin Solid Films 517 (2008) 750–754.

[4] V. Sharma, P. Kumar, J. Shrivastava, A. Solanki, V.R. Satsangi, S. Dass, R. Shrivastav, Synthesis and characterization of nanocrystalline $Zn_{1-x}M_xO$ (M = Ni, Cr) thin films for efficient photoelectrochemical splitting of water under UV irradiation, Int. J. Hydrog. Energy 36 (2011) 4280–4290.

[5] Y.R. Park, K.J. Kim, Sol–gel preparation and optical characterization of NiO and $Ni_{1-x}Zn_xO$ thin films, J. Cryst. Growth 258 (2003) 380–384.

[6] R. Noonuruk, W. Techitdheera, W. Pecharapa, Characterization and ozone-induced coloration of ZnxNi1−xO thin films prepared by sol–gel method, Thin Solid Films 520 (2012) 2769–2775.

[7] L. Herissi, L. Hadjeris, N. Attaf, M. S. Aida, A. Hafdallah, W. Daranfad, Réalisation et étude de couches minces de ZnO transparentes et conductrices, Alger. J. Adv. Mater. 4 (2008) 415–418.

[8] M. Karunakaran, R. Chandramohan, S. Balamurali, S. Gomathi, K. Kabila, T. Mahalingam, Structural and optical prosperities of nickel doped zinc oxide thin films grown by low cost modified SILAR method, Int. J. Thin Fil. Sci. Tec. 3-2 (2014) 61–65.

[9] S. Yılmaz, E. McGlynn, E. Bacaksız, J. Cullen, R.K. Chellappan, Structural, optical and magnetic properties of Ni-doped ZnO micro-rods grown by the spray pyrolysis method, Chem. Phys. Lett. 525–526 (2012) 72–76.

[10] S. Thakur, J. Kumar, J. Sharma, N. Sharma, P. Kumar, Structural and optical study of nickel doped ZnO nanoparticles and thin films for dye sensitized solar cell applications, J. Optoelectron. Adv. Mater. 15 (2013) 989–994.

[11] J.P. Mathew, G. Varghese, J. Mathew, Structural and optical properties of Ni:ZnO thin films-effect of annealing and doping concentration, Sop Trans. Appl. Phys. 1 (2014) 27–36.

[12] L. Mustafa, S. Anjum, S. Waseem, S. Bashir, K. Mahmood, M. Saleem, E. Ahmad, Structural and optical properties of ZnO co-doped with Co and Ni thin films deposited by pulse laser deposition technique, Opt. 161 (2018) 54–63.

[13] M. El-Hilo, A.A. Dakhel, A.Y. Ali-Mohamed, Room temperature ferromagnetism in nanocrystalline Ni-doped ZnO synthesized by co-precipitation, J. Magn. Magn. Mater. 321 (2009) 2279–2283.

[14] S. Aydogu, M.B. Coban, G. Cabuk, Influence of doping fluorine on the structural, surface morphological and optical properties of CdO films, Appl. Phys. A 123 (2017) pp409–11.

[15] M. Caglar, Y. Caglar, S. Ilican, The determination of the thickness and optical constants of the ZnO crystalline thin film by using envelope method, J. Optoelectron. Adv. Mater. 8 (2006) 1410–1413.

[16] L. Hadjeris, L. Herissi, M. Benbouzid, N. Attaf, M.B. Assouar, T. Easwarakhanthan, M.S. Aida, J. Bougdira, A. Mahdjoub, Structural, optical and electrical characterization of transparent and semiconducting ZnO thin films grown by spray pyrolysis, Alger. J. Adv. Mater. 4 (2008) 9–12.

[17] F. Ynineb, A. Hafdallah, M.S. Aida, N. Attaf, J. Bougdira, H. Rinnert, S. Rahmane, Influence of Sn content on properties of ZnO:SnO_2 thin films deposited by ultrasonic spray pyrolysis, Mater. Sci. Semicond. Process. 16 (2013) 2021–2027.

[18] L. Hadjeris, L. Herissi, M.B. Assouar, T. Easwarakhanthan, J. Bougdira, N. Attaf, M.S. Aida, Transparent and conducting ZnO films grown by spray pyrolysis, Semicond. Sci. Technol. 24 (2009) pp 035006–6.

[19] R. Mariappan, V. Ponnuswamy, P. Suresh, Effect of doping concentration on the structural and optical properties of pure and tin doped zinc oxide thin films by nebulizer spray pyrolysis (NSP) technique, Superlattices Microstruct. 52 (2012) 500–513.

[20] R. Swanepoel, Determination of the thickness and optical constants of amorphous silicon, J. Phys. E: Sci. In strum. 16 (1983) 1214–1222.

[21] E.R. Shaaban, I.S. Yahia, E.G. El-Metwally, Validity of Swanepoel method for calculating the optical constants of thick films, Acta Phys. Polonica A, 121 (2012) 628–635.

[22] P. Puspharajah, S. Radhakrishna, A. K. Arof, Transparent conducting lithium-doped nickel oxide thin films by spray pyrolysis technique, J. Mater. Sci. 32(1997) 3001–3006.

[23] H. Kamal, E.K. Elmaghraby, S.A. Ali, K. Abdel-Hady, Characterization of nickel oxide films deposited at different substrate temperatures using spray pyrolysis, J. Cryst. Growth 262 (2004) 424–434.

[24] L. Cattin, B.A. Reguig, A. Khelil, M. Morsli, K. Benchouk, J.C. Bernède, Properties of NiO thin films deposited by chemical spray pyrolysis using different precursor solutions, Appl. Surf. Sci. 254 (2008) 5814–5821.

[25] S. Singh, N. Rama, M.S.R. Rao, Influence of d-d transition bands on electrical resistivity in Ni doped polycrystalline ZnO, Appl. Phys. Lett. 88 (2006) pp 222111–3.

[26] I. Miccoli, F. Edler, H. Pfnür, C. Tegenkamp, The 100th anniversary of the four-point probe technique: the role of probe geometries in isotropic and anisotropic systems, J. Phys.: Condens. Matter. 27 (2015) pp 223201–29.